Communications in Physics, Vol. 34, No. 4 (2024), pp. 389-398
DOI: https://doi.org/10.15625/0868-3166/21404

# Insights into the structural, electronic and magnetic properties of gold clusters: Comparison between $Au_{12}Cr$ and $Au_{12}Mo$ clusters

**Ngo Thi Lan**[1,2,†], **Nguyen Van Dang**[1,‡], **Nguyen Thi Mai**[2], **Phung Thi Thu**[3], **Phan Thanh Phuong**[1], **Tran Xuan Quy**[1], **Le Thi Tuyet Ngan**[1], **Nguyen Thi Dung**[1] **and Nguyen Thanh Tung**[2]

[1]*TNU-University of Sciences, Tan Thinh Ward, Thai Nguyen City, Vietnam*

[2]*Institute of Materials Science, Vietnam Academy of Science and Technology, Hanoi, Vietnam*

[3]*University of Science and Technology of Hanoi, Vietnam Academy of Science and Technology, 18 Hoang Quoc Viet, Hanoi, Vietnam*

*E-mail:* †lannt@tnus.edu.vn; ‡dangnv@tnus.edu.vn

*Received 27 August 2024*; *Accepted for publication 8 November 2024*
*Published 27 November 2024*

**Abstract.** *Modification of the chemical and physical properties with respect to element components in atomic clusters has opened up significant potential in both fundamental study and applications. In this work, we theoretically investigate the structure, stability, and magnetic properties of gold clusters doped by Cr and Mo ($Au_{12}Cr$ and $Au_{12}Mo$) using the density functional theory calculation. The bond strength of AuM dimers dictates the globally minimum structural evolution in the $Au_{12}M$ clusters, which can be classified into two principal forms: the icosahedral (Mo dopant) and the cone-like structures (Cr dopant). The average binding and dissociation energies results indicate that the enhanced stability of cluster stems from the contribution of Cr/Mo atom. However, their magnetic moments are entirely distinct. To gain insight and a better understanding of the electronic configuration and magnetic behavior of the study clusters, the molecular orbital diagram and the spin distribution are computed. The $Au_{12}Cr$ cluster exhibits a significant magnetic moment of 4 $\mu_B$, whereas the magnetic moment is completely quenched in the $Au_{12}Mo$ cluster. Furthermore, the infrared IR spectrum of $Au_{12}M$ is also predicted.*

Keywords: $Au_{12}Cr$, $Au_{12}Mo$ clusters; density functional theory; magnetic moment.
Classification numbers: 31.15.xv; 31.15.E-; 75.30.-m; 81.07.-b.

## 1. Introduction

Much attention has dedicated to gold clusters in the recent decades thanks to their intriguing chemicophysical characteristics, such as magnetism, optics, catalysis, and electronic behavior, with a great potential in nanotechnology, electronics, and materials science [1–7]. Both theoretical and experimental investigations have revealed that the composition, shape, size, and charge state of the gold clusters have been considered as key factors for modifying their properties. Pure clusters behave as a non-magnetic material, while the appearance of the transition metal atom triggers the magnetic state in the cluster [8–10]. The unfilled 3*d* electrons of the transition metal dopant atoms have been demonstrated to play a crucial role in the unusual stability and distinctive properties of doped gold clusters. The hybridization between the *s*-delocalized electrons of the host and *d*-localized electrons of dopant atoms generates different electronic structures, resulting in a significant effect on the geometric structure and characteristics. Yang and colleagues [11] indicated the close correlation between the geometric, electronic structure and magnetic properties of $Au_{24}M$ clusters (M = V-Ni), as well as the valence electron configuration of the transition metal atom. The electronic structure based on a confined electron gas in a spherical structure complied with the jellium model was proposed by Knight et al. [12], forming cage-like structures with a large magnetic of 3 $\mu_B$ to 6 $\mu_B$. In this instance, the 3*d* transition metal atoms preferentially occupy positions with higher coordination numbers, typically located at the center of the cage. The effect of hybridization between valence electrons of the vanadium atom and those of noble clusters ($Au_n$, $Ag_n$, and $Cu_n$) has been found to play a significant role in stability and magnetic properties [13,14]. On the other hand, the electronic structure evolution of the $Au_{19}M$ (M = Sc-Ni) clusters has been explained by Tam and colleagues to follow the $1S^2 1P^6 1D^{10}$ filling rule [15, 16]. This suggests that the geometric structure of the $Au_{19}M$ clusters grows in accordance with a highly symmetric tetrahedral pyramid shape. The $Au_{19}Cr$ cluster is utterly stable and high magnetic moment of 5 $\mu_B$. A similar picture is also observed in $Au_9M^{2+}$ (M = Sc-Ni) clusters [17]. The remarkable influence of the position Fe atom on the electronic structure and magnetization of $Au_{18}Fe$ and $Au_{19}Fe$ clusters has been the subject of intensive investigation by Ehlert [18].

It is noticed that the 4*d* transition metal atoms exhibit more stable and filled electron configurations in various energy levels, stabilities, oxidation states, and chemical properties than the 3*d* transition metal atoms. When the group 3*d* and 4*d* atoms are attended in the gold clusters, their electronic structure differences result in distinct bonding patterns, spatial arrangements, and structural motifs [19]. The endohedral gold clusters containing ten gold atoms $Au_{10}W$ with large HOMO-LUMO gap, high ionization potential and electron affinities suggest that these clusters are all likely to be stable chemically, which is similar to the super-halogen $Al_{13}$ [20]. The existence of icosahedral 18-electron clusters $Au_{12}W$ was predicted theoretically [21] and found experimentally [22]. Anionic icosahedral 18-electron clusters $Au_{12}Ta^-$ and $Au_{12}Re^+$ were predicted theoretically [22]. These are explained by the hybridization of 1S, 1P, and 1D molecular orbitals in dopant nanoclusters. There is a contribution from the 12 valence electrons of the 6*s*-Au and six valence electrons from the dopant atoms. Juarez. L. F. Da Silva et al. [23] shown different trends in the structure and electronics of the 3*d* and 4*d* metal clusters containing 13 atoms by an effective coordination increase in large *d* state occupation. This comparative study provides insight into how the occupation of the *d* states influences the structural and electronic characteristics of these bimetallic systems.

It can be observed that gold clusters doped a transition metal atom provides opportunities to combine diverse geometric structures and unique properties of clusters with different electronic configurations. Therefore, this work investigates and compares the electronic, geometric structure, and IR spectra of the lowest energy state $Au_{12}M$ (M = Cr and Mo) clusters using density functional theory (DFT) calculations. Surprisingly, we have found two contrasting characteristics in the behavior of doped transition metal atom in gold clusters. The magnetism of the doped 4*d* transition metal atom cluster is completely quenched, resembling the Kondo effects. Conversely, the doped clusters of 3*d* atoms exhibit a significant magnetic moment. The magnetic moment of dopant clusters is correlated with the *d*-state electron of transition metal atoms. These theoretical findings provide important insight into advanced nanomaterials as foundational knowledge for upcoming experimental investigations.

## 2. Computational method

The geometric and electronic structures of $Au_{12}M$ (M = Cr and Mo) clusters were carried out by DFT calculations in the Gaussian 09 package [24, 25]. In this study, the initial optimization of the guessed structures involved the usage of the TPSS functional combined with basis set of cc-pVDZ-pp for Au and cc-pVDZ for Cr/Mo atoms, respectively. The isomers with relative energies below 2.0 eV were considered for further calculations. These selected isomers underwent single-point energies calculations using the same functional, but combining with larger basis sets, including cc-pVTZ-pp for Au and cc-pVTZ for Cr/Mo atoms, which based on previous investigations [26]. The functional selection is also based on test calculations for $Au_2$, AuCr, and AuMo dimers. These calculated results are presented in Table 1, along with available computational and experimental data for comparison. A self-consistent approach was employed with the convergence criteria of 2 x $10^{-5}$ Hartree for energy and 5.0 x $10^{-3}$ Å for displacement. The optimization calculations were followed by frequent calculations to identify the cluster's energy-minimized structure. The electronic configurations of ground-state clusters $Au_{12}M$ (M = Cr and Mo) were explored by using molecular diagram (MO) and spin density. The total/local magnetic moments (TMMs/LMMs) were defined as the difference between the numbers of spin-up and spin-down electrons occupying the molecular/atomic orbitals of the cluster/atom.

**Table 1.** Theoretical and experimental results of bond length $R_e$ (Å) and dissociation energy $D_e$ (eV) for $Au_2$, AuCr, and AuMo clusters.

| Clusters | | TPSSTPSS | PBEPBE | BP86 | Expt./others calculation |
|---|---|---|---|---|---|
| $Au_2$ | $R_e$ | 2.51 | 2.52 | 2.52 | 2.47 |
| | $D_e$ | 2.28 | 2.29 | 2.27 | 2.29 ± 0.008 [27] |
| AuCr | Re | 2.46 | 2.47 | 2.46 | |
| | $D_e$ | 2.26 | 2.23 | 2.35 | 2.29 ± 0.30 [27] |
| AuMo | $R_e$ | 2.54 | 2.54 | 2.58 | 2.55 [28] |
| | $D_e$ | 2.27 | 2.28 | 2.29 | 2.26 [28] |

## 3. Results and discussion

### *3.1. The optimal geometric and spin multiplicities*

The effects of 3*d* and 4*d* transition metal atoms on pure gold clusters $Au_{13}$ were investigated by means of the optimization process of geometrical and electronic structures. Firstly, the $Au_{13}$ cluster was computed to find the most stable geometric structure. Next step is the replacement of an Au atom in the $Au_{13}$ cluster by a Cr or Mo atom at all feasible positions to generate initial $Au_{12}M$ structures for the optimization calculations. Noticeably, there are several low-lying isomers and corresponding spin configurations for each $Au_{12}M$ (M = Cr and Mo), which satisfies convergent condition. Nevertheless, only the structures with lowest energy considered as the ground-state configuration are discussed. They are displayed in Fig. 1 for both $Au_{12}Cr$ and $Au_{12}Mo$ clusters. Comparing to previous articles, our calculations results are in a complete agreement with those published findings [29]. In the following, the isomers with increasing order of energy are donated as A, B, and C. Additionally, information regarding the spin multiplicities and energy differences compared to each ground-state structure is also presented.

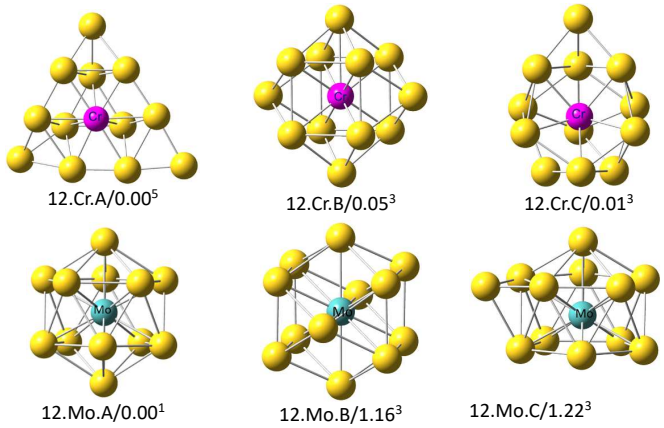


**Fig. 1.** Optimized structures, spin multiplicities, and relative energies (in eV) of the lowest lying isomers of $Au_{12}M$ (M = Cr and Mo). The yellow, magenta, and blue balls show Au, Cr and Mo atom, respectively.

The significant difference in geometric structure and spin multiplicities is observed in the gold clusters, corresponding to 3*d* (Cr) and 4*d* (Mo) transition metal dopants. The $Au_{12}Mo.A$ cluster shows the perfect icosahedral cage structure with singlet spin, while the $Au_{12}Cr.A$ has a cone-like structure and higher spin of quintet, which can be attributed to Jahn-Teller effects. Structural rearrangement occurred at different isomers corresponding to higher energies. In addition to the change of geometry from the cone-like shape ($Au_{12}Cr.A$) to dodecahedral structure ($Au_{12}Cr.B$), the Cr atom moves from the face to the center of the frame. The difference in energy between $Au_{12}Cr.B$ and the ground-state $Au_{12}Cr.A$ is 0.05 eV. The relative energy of the unstable triplet $Au_{12}Cr.C$ is higher than the ground-state by 0.1 eV, and the geometry again tends to retain a layered motif with a substituted dopant atom on the surface center. At this energy, the pin-like structure in bowling game is grown in the $Au_{12}Mo.C$. Conversely, higher relative energy levels are

required to evolve the $Au_{12}$Mo.B and $Au_{12}$Mo.C structures. The transformation from the high-symmetry icosahedral to hexagonal-like structure according to the energy difference of 1.16 eV or to more complex polygonal shape in the least unstable cluster (the energy difference of 1.22 eV) is observed. However, the central position of Mo dopant atom is preserved in three configurations.

The difference in the shape of $Au_{12}$M (M = Cr and Mo) can be explained by the differences in the binding energy (BE) of AuM and $Au_2$. The calculations point out that the Au-Mo (1.15 eV) bond is stronger than that of Au-Au (1.13 eV), this value is similar in the case of Au-Cr (1.13 eV). This confirmed that the Mo atom favors the high position compared with Cr atoms. A similar behavior was reported for $Ag_{12}$Cr in the previous studies [29, 30]. In that system, the binding energy (BE) of Ag-Ag bonds (0.81 eV) is higher than the BE of Ag-Cr bonds (0.73 eV). As a result of this difference in the binding energies, the Cr atom is substituted by an Ag atom in the central icosahedral structure.

### *3.2. Stabilities*

To evaluate how the transition metal dopant atom affects the stability of the clusters, the average BE is calculated and then compared to that of the pure gold clusters $Au_{13}$. The BE values are determined by the following formulas:

$$BE(Au_{12}M) = \frac{1}{13}[E(M) + 12\mathrm{E(Au)} - \mathrm{E(Au_{12}M)}, \quad (1)$$

$$BE(Au_{13}) = \frac{1}{13}[13E(Au) - \mathrm{E(Au_{13})}, \quad (2)$$

where E(M), E(Au), E($Au_{13}$), and E($Au_{12}$M) correspond the total energies of M, Au atoms, and the $Au_{13}$, $Au_{12}$M clusters. Visibly, the binding energy values of doped clusters are significantly higher than the BE of pure counterpart, BE ($Au_{12}$Cr) of 2.24 eV and BE ($Au_{12}$Mo) of 2.49 eV compared to BE ($Au_{13}$) of 2.0 eV, as shown in Table 1. It can be concluded that the role of Cr and Mo atoms enhance the stability of Au clusters. An analogous picture was also obtained for $Au_9M^{2+}$ (M = Sc-Ni) clusters [17] in which the estimated atomic-averaged binding energy of the most stable $Au_9Cr^{2+}$ was substantially higher than that of $Au_{10}{}^{2+}$cluster. This trend is also observed in gold clusters doped 4*d* transition metal atoms $Au_{n\text{-}1}$Y. The global structure with the Y atom has the highest number of neighboring Au atoms because the Au-Y bond strength is stronger than that of the Au-Au bond [31].

**Table 2.** The binding energy per atom (BE in eV), dissociation energies (DE in eV), and bond length ($R_{M\text{-}Au}$ in Å) of $Au_{13}$ and $Au_{12}$M clusters.

| **Clusters** | **BE (eV)** | **DE (eV)** | |
|---|---|---|---|
| | | **loss Au** | **loss M** |
| $Au_{13}$ | 2.0 | 1.75 | - |
| $Au_{12}$Cr | 2.24 | 2.75 | 3.13 |
| $Au_{12}$Mo | 2.49 | 4.83 | 6.56 |

Furthermore, we also consider dissociation energies (DE in eV) in order to understand the influence of the M atom on the thermodynamic stability of $Au_{12}$M (M = Cr and Mo) structure.

The fragmentation of $Au_{12}M$ cluster via two major possible channels was calculated, including a loss of a M atom, and an Au atom. The formulas for calculating the DE are expressed as follows:

$$\mathrm{DE(M)} = \mathrm{E(Au_{12})} + \mathrm{E(M)} - \mathrm{E(Au_{12}M)}, \quad (3)$$

$$\mathrm{DE(Au)} = \mathrm{E(Au_{11}}M) + \mathrm{E(Au)} - \mathrm{Au_{12}M}, \quad (4)$$

where E represents the energy of the atom/cluster. The dissociation energies are presented in the Table 2 as well, which are defined as the energetic difference between the total electronic energies of the species generated in each dissociation channel and the electronic energies of the parent clusters. Obviously, the loss of an Au atom is the most energetically preferred dissociation channel, whereas the other channel to decay a M atom requires a higher energy. Compared to $Au_{12}Cr$, the dissociation energies of both channels in the $Au_{12}Mo$ are significantly higher, indicating more stable $Au_{12}Mo$ structure. This result is very consistent with the average binding energy.

### *3.3. Electronic and magnetic properties*

As well known, Cr and Mo are strong magnetic elements with outermost atomic shell of $3d^5 4s^1$ and $4d^5 5s^1$, respectively. However, doping Cr or Mo atoms into gold clusters results in a completely different scenario. Typically, the magnetism in $Au_{12}Mo$ is entirely quenched, yet the $Au_{12}Cr$ cluster shows non-zero magnetic state of 4 $\mu_B$. In this regard, our objective is to investigate the fundamental physics to explain the distinction between these clusters. Additionally, determination whether if the possibility to develop a universal mechanism for predicting the magnetic behavior in analogous quantum systems is a fascinating finding. It is worth mentioning that substituting different transition metal impurity atoms while maintaining the host clusters intact results in different significant variations of properties in the dopant systems. Particularly, the lowest-lying isomer of $Au_{12}Cr$ favor in the cone shape, whereas $Au_{12}Mo$ is icosahedral cage for comparison, as mentioned above. As a consequence, their electronic configurations display a remarkable difference [32–34]. The electronic shell structure formation in these clusters can be explained by the interactions between the delocalized *(s)* and localized *(d)* electrons. It assumes that each gold atom delocalizes its $6s^1$ electron, while the Cr and Mo atoms collectively contribute 6 valence electrons from the configurations of $3d^5 4s^1$ and $4d^5 5s^1$, respectively. As a result, the $Au_{12}Cr$ and $Au_{12}Mo$ will provide a total of 18 valence electrons. A graphical representation of their corresponding molecular orbital diagram was plotted to get more clear clarity on the electronic shell structure of the clusters, as seen in Fig 2. By examining the molecular orbitals (MOs) and their orbital energy levels for the $Au_{12}Cr$ and $Au_{12}Mo$, it can be observed significant differences, which serve as an indicator of distinct variations in their electronic thermochemical stability. In the case of the $Au_{12}Mo$ cluster, there is strong hybridization of 6*s* orbital of Au and the *sd* orbitals of Mo, leading to the delocalization of all six valence electrons of Mo ($4d^5 5s^1$), which then combine with twelve *s* valence electrons of the Au host. This process results in the complete filling of the $1S^2 1P^6 1D^{10}$ orbitals, forming a closed shell configuration and a stable structure. Consequently, the Mo dopant exhibits a quenched magnetic moment. In analogy to $Cu_{12}Cr$, Mai and et al., have observed the completely magnetic quenching in the $Cu_{12}Cr$ which the valence electrons fulfill the 18-electrons counting rule ($3d^5 4s^1$) for Cr atom and twelve $5s^1$ electrons for copper atoms [29].

On the other hand, only two delocalized electrons of 4*s*-Cr join in twelve electrons of the Au host cluster, forming electronic shell structure of $1S^2 1P^6 1D^6$. The remaining 4 electrons are localized on 3*d*-Cr atomic orbitals, responding to the magnetic properties. The magnetic moment

of $Au_{12}Cr$, therefore, originated from the co-existence of delocalized electron shell and localized magnetic shell. It turns out that the electronic configuration of the $Au_{12}Mo$ and $Au_{12}Cr$ clusters basically satisfies the electronic shell model of $1S^2 1P^6 1D^{10}$ and $1S^2 1P^6 1D^6 3d^4{}_{\uparrow}$ with completely quenched and 4 $\mu_B$ magnetic moments, respectively.

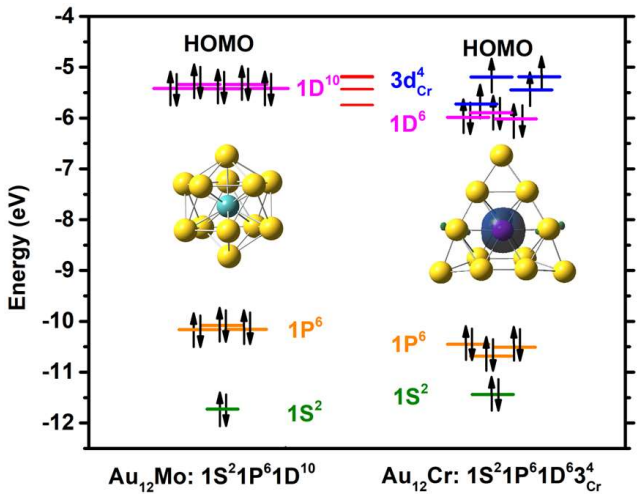


**Fig. 2.** The MO diagram of $Au_{12}Mo$ (left) and $Au_{12}Cr$ (right) clusters.

It can be seen that the magnetism of $Au_{12}Mo$ and $Au_{12}Cr$ depends on the hybridization of 3*d* dopant electrons and *s* host electron. To understand more about the magnetic properties of studied clusters, we analyzed the local magnetic moment (LMM) and total magnetic moments (TMM) in $\mu_B$. The magnetic moment of 3*d*/4*d*-M (M = Cr and Mo), 6*s*-Au and total magnetic moment (in $\mu_B$) of $Au_{12}M$ are shown in Table 3. Regarding the $Au_{12}Mo$, the 4*d* local magnetic moment of Mo and 6*s* of Au is zero. This result aligns with the molecular orbital diagram, which indicates the pairing of Mo and Au valence electrons within the molecular shell. Compared with the $Au_{12}Mo$, the $Au_{12}Cr$ is more interesting. The LMM in the 3*d* orbitals of Cr is 3.6 $\mu_B$, while that of 6*s* orbital of Au is only 0.01 $\mu_B$. In other words, the TMM of clusters is predominantly contributed by the LMM of 3*d*-atom.

**Table 3.** Local magnetic moments (LMM in $\mu_B$) of Cr/Mo atom, and total magnetic moment (TMM in $\mu_B$) of $Au_{12}Cr$ and $Au_{12}Mo$, respectively.

| $Au_{12}M$ | **LMM ($\mu$B)** | | | | **TMM ($\mu$B)** |
|---|---|---|---|---|---|
| | $3d/4d-M$ | $4s/5s-M$ | $4p/5p-M$ | $6s-Au$ | |
| $Au_{12}Cr$ | 3.60 | 0.03 | 0.04 | 0.01 | 4 |
| $Au_{12}Mo$ | 0 | 0 | 0 | 0 | 0 |

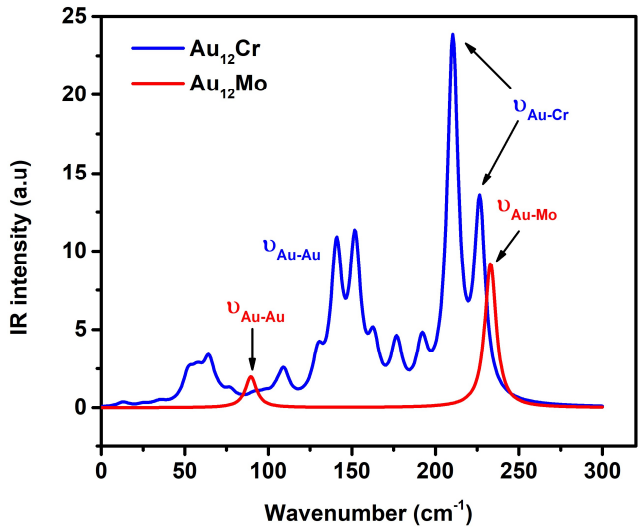


**Fig. 3.** IR spectra for $Au_{12}M$ (M = Cr and Mo) clusters. The blue and red curves represent the IR spectrum of $Au_{12}Cr$ and $Au_{12}Mo$ clusters, respectively.

### *3.4. IR spectra of the investigated clusters*

In this subsection, we investigate the IR spectra of the most stable structure. The infrared IR spectrum provides valuable information and insight into molecular structure and vibrational modes. Theoretical research results on IR spectra play a crucial role in advancing further studies, especially in experimental investigations, assisting in the accurate determination of cluster structures during synthesis. However, no information about the infrared IR spectrum of $Au_{12}M$ clusters has been reported both experimentally and theoretically so far. Therefore, the IR spectra of $Au_{12}M$ (M = Cr and Mo) are regarded as a first fingerprint for identifying the cluster with respect to the geometrical structure and composition of M atoms. For the purpose of comparison in order to help distinguish the two dopant atoms, $Au_{12}$ Cr and $Au_{12}Mo$ clusters, the calculated IR spectra. Fig. 3 displays the IR spectra of $Au_{12}Cr$ and $Au_{12}Mo$ with the range from 0 to 300 $cm^{-1}$ because no detectable signals were observed at higher photon energy levels. The peaks corresponding to higher frequencies (> 210 $cm^{-1}$) are represented the vibrations of the Cr/Mo atoms within the $Au_{12}$ host framework, while the lower frequency peaks characterize the vibration of Au-Au bonds. This picture shows good agreement for the neutral dimer Au-Au vibration at a frequency of 190.0 $cm^{-1}$ [35]. According to the IR spectra and experimental findings, the vibration $Au_{12}$ is also observed at frequency of less than 200 $cm^{-1}$ [36]. As can be seen in Fig 3, the vibrational spectra in the icosahedral $Au_{12}Mo$ structure only exhibits two high intense peaks. The highest peak, located at ~234 $cm^{-1}$ is characteristic of the symmetric stretching mode of Mo- Au bonds. The lower peak at ~91 $cm^{-1}$ corresponds to the symmetric stretching vibrations of Au-Au bonds. In other words, the lowest-lying structure of $Au_{12}Mo$ clusters is utterly high symmetry with icosahedral shape. In contrast to the IR spectra of the $Au_{12}Mo$, the IR spectra of $Au_{12}Cr$ cluster is more complicated, characterized by multiple peaks. Considering the distorted cone shaped $Au_{12}Cr$ spectrum, it can be observed two asymmetric stretching modes of Cr-Au bonds at high frequencies: ~210 $cm^{-1}$

and ~227 $cm^{-1}$. The peaks at ~110 $cm^{-1}$, ~141 $cm^{-1}$ and ~163 $cm^{-1}$ are assigned to the symmetric stretching of Au-Au bonds. Conversely, the asymmetric stretching modes of Au-Au bonds are assigned at ~ 64 $cm^{-1}$, ~110 $cm^{-1}$, ~130 $cm^{-1}$, ~152 $cm^{-1}$ and ~177 $cm^{-1}$.

## 4. Conclusion

The geometric and electronic structures, stability, and magnetic properties of the 13-atom gold cluster doped with 3*d* and 4*d* transition metal atoms, $Au_{12}M$ with M = Cr and Mo were investigated using DFT methods. The most stable isomer of $Au_{12}Cr$ favors a cone-like shape, and the $Au_{12}Mo$ structure prefers an icosahedral structure with Mo located in the center. The electronic shell of $Au_{12}Mo$ is filled with a magic number of 18 valence electrons, which has a perfect icosahedral structure, and enjoy enhanced stability with high binding and dissociation energies. Their higher stability can be interpreted in terms of the electronic shells of the jellium model. The magnetic moment of the clusters has been demonstrated to be proportional to the number of unpaired electrons that are localized on the 3*d*-M orbitals. This finding opens up an avenue for how chemically inert gold clusters can be adjusted magnetically by a suitable transition metal impurity. The IR spectra of $Au_{12}M$ are simulated to provide valuable guidance for future experimental assignments of these ground-state bimetallic systems.

## Acknowledgment

This research was financially supported by National Foundation of Science and Technology Development (NAFOSTED) under the grant number 103.01-2021.109.

## Conflict of interest

The authors have no conflicts of interest to declare.

## References

[1] V. Yarzhemsky, Y. A. D'yakov, A. Izotov, and V. Izotova, *Chemical Properties of Gold Clusters as Dependent on the Structure and Doping by 5d Elements*, Russ. J. Inorg. Chem. **64** (2019) 1242.

[2] Y. Sun, X. Liu, K. Xiao, Y. Zhu, and M. Chen, *Active-site tailoring of gold cluster catalysts for electrochemical $CO_2$ reduction*, ACS Catal. **11** (2021) 11551.

[3] H. Cui, Z. S. Shao, Z. Song, Y. B. Wang, and H. S. Wang, *Development of gold nanoclusters: From preparation to applications in the field of biomedicine*, J. Mater. Chem. C **8** (2020) 14333.

[4] S. Zhu, X. Wang, Y. Cong, and L. Li, *Regulating the optical properties of gold nanoclusters for biological applications*, ACS Omega **5** (2020) 22702.

[5] D. Cheng, R. Liu, and K. Hu, *Gold nanoclusters: Photophysical properties and photocatalytic applications,* Front. Chem. **10** (2022) 958626.

[6] S. M. V. Looij, E. R. Hebels, M. Viola, M. Hembury, S. Oliveira, and T. Vermonden, *Gold nanoclusters: imaging, therapy, and theranostic roles in biomedical applications*, Bioconjug. Chem. **33** (2021) 04.

[7] Y. Gao, N. Shao, Y. Pei, Z. Chen, and X. C. Zeng, *Catalytic activities of subnanometer gold clusters ($Au_{16}$-$Au_{18}$, $Au_{20}$, and $Au_{27}$-$Au_{35}$) for CO oxidation*, ACS nano **5** (2011) 7818.

[8] D. Dong, K. Xiao-Yu, Z. Bing, and G. Jian-Jun, *Geometrical, electronic, and magnetic properties of small $Au_nSc$ (n= 1–8) clusters*, Phys. B: Condens. Matter **406** (2011) 3160.

[9] B. Zhu, D. Die, R. C. Li, H. Lan, B. X. Zheng, and Z. Q. Li, *Insights into the structural, electronic and magnetic properties of Ni-doped gold clusters: Comparison with pure gold clusters*, J. Alloys Compd. **696** (2017) 402.

[10] X. Li, B. Kiran, L. F. Cui, and L. S. Wang, *Magnetic properties in transition-metal-doped gold clusters: $MAu_6$ (M= Ti, V, Cr)*, Phys. Rev. Lett. **95** (2005) 253401.

[11] A. Yang, W. Fa, and J. Dong, *Magnetic properties of transition-metal-doped tubular gold clusters: $MAu_{24}$ (M= V, Cr, Mn, Fe, Co, and Ni)*, J. Phys. Chem. A **114** (2010) 4031.

[12] W. Knight, K. Clemenger, W. A. De Heer, W. A. Saunders, M. Chou, and M. L. Cohen, *Electronic shell structure and abundances of sodium clusters*, Phys. Rev. Lett. **52** (1984) 2141.

[13] W. H. Blades, A. C. Reber, S. N. Khanna, L. López-Sosa, P. Calaminici, and A. M. Köster, *Evolution of the Spin Magnetic Moments and Atomic Valence of Vanadium in $VCu_x^+$, $VAg_x^+$, and $VAu_x^+$ Clusters (x = 3–14)*, J. Phys. Chem. A **121** (2017) 2999.

[14] P. Ranjan, and T. Chakraborty, *A DFT study of vanadium doped gold nanoalloy clusters*, Key Eng. Mater. **777** (2018) 183.

[15] N. M. Tam, N. T. Cuong, H. T. Pham, and N. T. Tung, *$Au_{19}M$ (M= Cr, Mn, and Fe) as magnetic copies of the golden pyramid*, Sci. Rep. **7** (2017) 16086.

[16] N. M. Tam, N. T. Mai, H. T. Pham, N. T. Cuong, and N. T. Tung, *Ultimate Manipulation of Magnetic Moments in the Golden Tetrahedron $Au_{20}$ with a Substitutional 3d Impurity*, J. Phys. Chem. C **122** (2018) 16256.

[17] N. T. Lan, N. T. Mai, D. D. La, N. M. Tam, S. T. Ngo, and N. T. Tung, *DFT investigation of $Au_9M^{2+}$ nanoclusters (M= Sc-Ni): The magnetic superatomic behavior of $Au_9Cr^{2+}$*, Chem. Phys. Lett. **793** (2022) 139451.

[18] C. Ehlert, and I. P. Hamilton, *Iron doped gold cluster nanomagnets: ab initio determination of barriers for demagnetization*, Nanoscale Adv. **1** (2019) 1553.

[19] Z. Meng, F. Xiao-Juan, Z. Li-Xia, H. Li-Ming, and L. You-Hua, *Density-functional investigation of 3d, 4d, 5d impurity doped $Au_6$ clusters*, Chin. Phys. B **19** (2010) 043103.

[20] D. Hossain, C. U. Pittman, and S. R. Gwaltney, *Structures and Stabilities of the Metal Doped Gold Nano-Clusters: $MAu_{10}$ (M= W, Mo, Ru, Co)*, J. Inorg. Organomet. Polymers Mater. **24** (2014) 241.

[21] P. Pyykkö, *Theoretical chemistry of gold*, Angew. Chem., Int. Ed. **43** (2004) 4412.

[22] V. Yarzhemsky, M. Kazaryan, Y. A. Dyakov, V. Izotova, and O. Kosheleva, *Structure and donor–acceptor properties of $Au_{12}M$ (M= Hf, Ta, W, Re, and Os) intermetallic clusters*, Russ. J. Inorg. Chem. **62** (2017) 72.

[23] M. J. Piotrowski, P. Piquini, and J. L. Da Silva, *Density functional theory investigation of 3 d, 4d, and 5 d 13-atom metal clusters*, Phys. Rev. B **81** (2010) 155446.

[24] M. Frisch, G. Trucks, H. Schlegel, G. Scuseria, Robb, and G.A. Pertersson, *Gaussian 09, Revision a. 02, 200, gaussian*, Inc., Wallingford, CT, **271** 2009.

[25] P. Hohenberg, and W. Kohn, *Inhomogeneous electron gas*, Phys. Rev. **136** (1964) B864.

[26] Q. Du, X. Wu, P. Wang, D. Wu, L. Sai, and J. Zhao, *Structure evolution of transition metal-doped gold clusters $MAu_{12}$ (M= 3d–5d): Across the periodic table*, J. Phys. Chem. C **124** (2020) 7449.

[27] M. D. Morse, *Clusters of transition-metal atoms*, Chem. Rev. **86** (1986) 1049.

[28] A. Ghassami, E. Oleiki, D. Y. Kim, H. J. Shin, G. Lee, and K. S. Kim, *Facile room-temperature self-assembly of extended cation-free guanine-quartet network on Mo-doped Au (111) surface*, Nanoscale Adv. **3** (2021) 3867.

[29] N. T. Mai, N. T. Lan, N. T. Cuong, N. M. Tam, S. T. Ngo, T. T. Phung, and N. T. Tung, *Systematic Investigation of the Structure, Stability and Spin Magnetic Moment of $CrM_n$ Clusters (M= Cu, Ag, Au, and n= 2–20) by DFT Calculations*, ACS Omega **6** (2021) 2034.

[30] N. T. Lan, N. T. Mai, B. S. Tung, N. Van Dang and N. T. Tung, *Structures, stabilities and infrared spectra of $Ag_nCr$ clusters (n= 2-12) by density functional theory calculation*, J. Military Science and Technology **77** (2022) 73.

[31] M. Hua-Ping, W. Hong-Yan and S. Yong, *Density functional study on structural and electronic properties of bimetallic gold–yttrium clusters: comparison with pure gold and yttrium clusters*, Chin. Phys. B **17** (2008) 2110.

[32] K. Clemenger, *Ellipsoidal shell structure in free-electron metal clusters*, Phys. Rev. B **32** (1985) 1359.

[33] W. A. De Heer, *The physics of simple metal clusters: experimental aspects and simple models*, Rev. Mod. Phys. **65** (1993) 611.

[34] M. Brack, *The physics of simple metal clusters: self-consistent jellium model and semiclassical approaches*, Rev. Mod. Phys. **65** (1993) 677.

[35] J. P. Merrick, D. Moran and L. Radom, *An evaluation of harmonic vibrational frequency scale factors*, J. Phys. Chem. A **111** (2007) 11683.

[36] B. R. Goldsmith, J. Florian, J. Liu, P. Gruene, J. T. Lyon and L. M. Ghiringhelli, *Two-to-three dimensional transition in neutral gold clusters: The crucial role of van der Waals interactions and temperature*, Phys. Rev. Mater. **3** (2019) 016002.